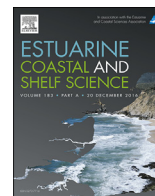




Contents lists available at ScienceDirect

## Estuarine, Coastal and Shelf Science

journal homepage: [www.elsevier.com/locate/ecss](http://www.elsevier.com/locate/ecss)

## Chemical and biological impacts of ocean acidification along the west coast of North America



Richard A. Feely<sup>a,\*</sup>, Simone R. Alin<sup>a</sup>, Brendan Carter<sup>b</sup>, Nina Bednaršek<sup>c,1</sup>, Burke Hales<sup>d</sup>, Francis Chan<sup>e</sup>, Tessa M. Hill<sup>f,g</sup>, Brian Gaylord<sup>f</sup>, Eric Sanford<sup>f</sup>, Robert H. Byrne<sup>h</sup>, Christopher L. Sabine<sup>a</sup>, Dana Greeley<sup>a</sup>, Lauren Juranek<sup>d</sup>

<sup>a</sup> NOAA Pacific Marine Environmental Laboratory, 7600 Sand Point Way NE, Seattle, WA 98115, USA

<sup>b</sup> Joint Institute for the Study of the Atmosphere and Ocean, University of Washington, Seattle, WA 98195, USA

<sup>c</sup> School of Marine and Environmental Affairs, University of Washington, Seattle, WA 98195, USA

<sup>d</sup> College of Oceanic and Atmospheric Sciences, Oregon State University, Corvallis, OR 97331, USA

<sup>e</sup> Department of Integrative Biology, Oregon State University, Corvallis, OR 97331, USA

<sup>f</sup> Bodega Marine Laboratory, University of California Davis, Bodega Bay, CA 94923, USA

<sup>g</sup> Department of Earth and Planetary Sciences, University of California Davis, Davis, CA 95616, USA

<sup>h</sup> College of Marine Science, University of South Florida, 140 7th Avenue South, St. Petersburg, FL 33701, USA

## ARTICLE INFO

## Article history:

Received 16 March 2016

Received in revised form  
12 July 2016

Accepted 29 August 2016

Available online 31 August 2016

## Keywords:

California current large marine ecosystem

Ocean acidification

Anthropogenic CO<sub>2</sub>

Upwelling

Pteropod dissolution

## ABSTRACT

The continental shelf region off the west coast of North America is seasonally exposed to water with a low aragonite saturation state by coastal upwelling of CO<sub>2</sub>-rich waters. To date, the spatial and temporal distribution of anthropogenic CO<sub>2</sub> (C<sub>anth</sub>) within the CO<sub>2</sub>-rich waters is largely unknown. Here we adapt the multiple linear regression approach to utilize the GO-SHIP Repeat Hydrography data from the northeast Pacific to establish an annually updated relationship between C<sub>anth</sub> and potential density. This relationship was then used with the NOAA Ocean Acidification Program West Coast Ocean Acidification (WCOA) cruise data sets from 2007, 2011, 2012, and 2013 to determine the spatial variations of C<sub>anth</sub> in the upwelled water. Our results show large spatial differences in C<sub>anth</sub> in surface waters along the coast, with the lowest values (37–55 μmol kg<sup>-1</sup>) in strong upwelling regions off southern Oregon and northern California and higher values (51–63 μmol kg<sup>-1</sup>) to the north and south of this region. Coastal dissolved inorganic carbon concentrations are also elevated due to a natural remineralized component (C<sub>bio</sub>), which represents carbon accumulated through net respiration in the seawater that has not yet degassed to the atmosphere. Average surface C<sub>anth</sub> is almost twice the surface remineralized component. In contrast, C<sub>anth</sub> is only about one third and one fifth of the remineralized component at 50 m and 100 m depth, respectively. Uptake of C<sub>anth</sub> has caused the aragonite saturation horizon to shoal by approximately 30–50 m since the preindustrial period so that undersaturated waters are well within the regions of the continental shelf that affect the shell dissolution of living pteropods. Our data show that the most severe biological impacts occur in the nearshore waters, where corrosive waters are closest to the surface. Since the pre-industrial times, pteropod shell dissolution has, on average, increased approximately 19–26% in both nearshore and offshore waters.

Published by Elsevier Ltd.

## 1. Introduction

Since the beginning of the Industrial Revolution, the global oceans have absorbed about 28% (~550 billion tons) of the total

anthropogenic carbon dioxide (CO<sub>2</sub>) emissions (Canadell et al., 2007; IPCC, 2013; Le Quéré et al., 2015). This absorption of atmospheric CO<sub>2</sub> has increased ocean acidity in a process referred to as “anthropogenic” ocean acidification (OA). Over the past 250 years, the pH of open-ocean surface waters has decreased by approximately 0.11 units, equivalent to an increase of about 28% in hydrogen ion concentration (Gattuso et al., 2015). When CO<sub>2</sub> enters the ocean, it reacts with water to form carbonic acid, which

\* Corresponding author.

E-mail address: [Richard.A.Feely@noaa.gov](mailto:Richard.A.Feely@noaa.gov) (R.A. Feely).

<sup>1</sup> Previously at NOAA Pacific Marine Environmental Laboratory, USA.

consumes carbonate ions ( $\text{CO}_3^{2-}$ ) via the release of protons. In direct correspondence with these changes, the  $\text{CO}_3^{2-}$  concentration has declined about 16% from preindustrial values through the year 2000. Under a “business-as-usual”  $\text{CO}_2$  emission scenario, surface ocean pH is expected to decline by another 0.3–0.4 units by the end of the century and  $\text{CO}_3^{2-}$  concentration is expected to decline by 50% over the same period (Feely et al., 2004, 2009; Orr et al., 2005; Doney et al., 2009a,b; IPCC, 2013; Gattuso et al., 2015).

Organisms that produce calcium carbonate ( $\text{CaCO}_3$ ) shells or skeletons made of aragonite or calcite are expected to encounter increasing physiological challenges as the saturation state of aragonite and calcite decreases due to OA (Fabry et al., 2008; Guinotte and Fabry, 2008; Hofmann and Todgham, 2010; Gaylord et al., 2011; Barton et al., 2012; Bednaršek et al., 2012a, 2014a,b; Hettinger et al., 2012; Frieder et al., 2014; Gattuso et al., 2015; Waldbusser et al., 2015; Somero et al., 2016). The saturation state of aragonite ( $\Omega_{\text{ar}}$ ) and calcite ( $\Omega_{\text{cal}}$ ) is a function of the concentrations of calcium ( $\text{Ca}^{2+}$ ) and  $\text{CO}_3^{2-}$ , and pressure-dependent stoichiometric solubility product,  $K_{\text{sp}}^*$ : ( $\Omega = [\text{Ca}^{2+}][\text{CO}_3^{2-}]/K_{\text{sp}}^*$ ) (Mucci, 1983), such that  $\Omega_{\text{ar}}$  and  $\Omega_{\text{cal}}$  will decline as more  $\text{CO}_2$  is taken up by the oceans. At  $\Omega = 1$ , carbonate minerals are in equilibrium with surrounding seawater; at  $\Omega > 1$ , precipitation or preservation of carbonate minerals is thermodynamically favored; and at  $\Omega < 1$ , dissolution is favored.

Recent models suggest that the shallower waters along the California Current Large Marine System (CCLME) will become undersaturated more often, and for longer durations, over the next several decades to a century (Gruber et al., 2012; Hauri et al., 2013; Turi et al., 2016). Persistence of acidified water in the coastal waters of the west coast of North America could have profound consequences for marine organisms, ecosystems, and the ecosystem services of this region (Doney et al., 2009a; Gattuso and Hansson, 2011; Feely et al., 2012a; Ekstrom et al., 2015; Gaylord et al., 2015; Somero et al., 2016). Increasing  $\text{CO}_2$  may have significant biological and ecological effects, with potential feedbacks to biogeochemical cycles. Declines in  $\text{CaCO}_3$  saturation state, particularly  $\Omega_{\text{ar}}$ , will pose increasing physiological challenges to calcifying invertebrates such as pteropods, bivalves, and echinoderms (Wootton et al., 2008; Hettinger et al., 2012; Kroeker et al., 2013; Frieder et al., 2014; Bednaršek et al., 2012a, 2014a,b; Waldbusser et al., 2015; Barton et al., 2015; Somero et al., 2016).

Pteropods are an important food source for organisms across lower (e.g. macrozooplankton) and higher trophic levels in the oceans. In the North Pacific Ocean, pteropods are seasonally substantial portion of the diets of pink and chum salmon (Groot and Margolis, 1991), sablefish and rock sole (Armstrong et al., 2005; Aydin et al., 2005). Moreover, they are among the species most affected by ocean acidification, with shell dissolution already occurring in the natural environment (Bednaršek et al., 2014a). Consequently, pteropods are ideal sentinel organisms to study how the dissolution changes since the pre-industrial times are affecting aragonite dissolution in the CCLME, and help to identify which of the regions are the most vulnerable to the anthropogenic changes. In this paper we estimate the amount of anthropogenic  $\text{CO}_2$  ( $C_{\text{anth}}$ ) in the CCLME region and determine its impact on pteropod shell dissolution comparatively for cruises in 2011 and 2013.

### 1.1. Physical and biogeochemical setting

The CCLME is a large-scale oceanographic feature along the west coast of North America, an eastern boundary current extending from northern Vancouver Island in Canada to Punta Eugenia in Mexico, and landward into large estuarine systems such as the San Francisco Bay and the Salish Sea (Fig. 1). The coastal waters off the west coast of North America are strongly affected by seasonal

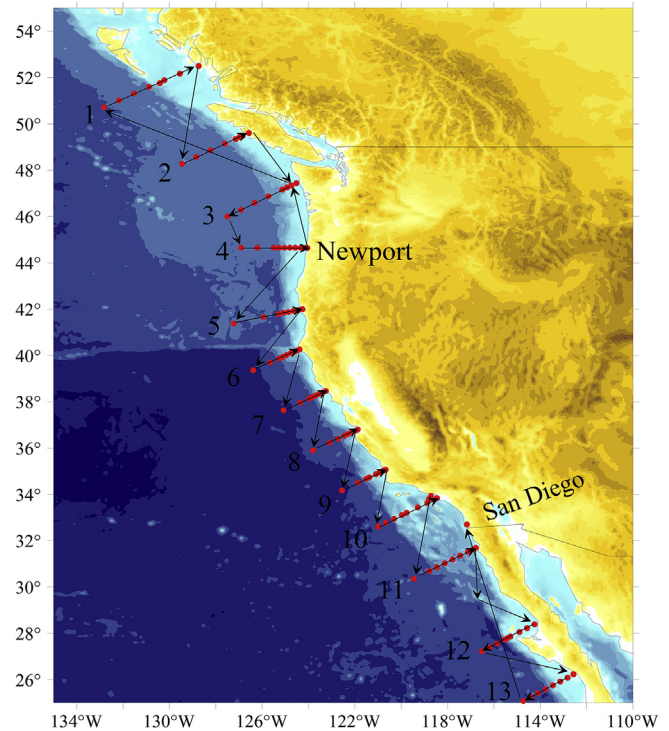


Fig. 1. Map of the station locations for the 2007 West Coast cruise. The black line shows the cruise track. The 2011, 2012, and 2013 cruises included subsets of these stations and, in some cases, a few additional stations.

upwelling, which typically begins in early spring when the Pacific High moves into the subarctic North Pacific, resulting in a strengthening of the northwesterly winds. These winds drive net surface waters offshore via Ekman transport, which induces the upwelling of low pH, nutrient- and  $\text{CO}_2$ -rich, intermediate depth (100–300 m) offshore waters onto the continental shelf (Hales et al., 2006; Feely et al., 2008; Gruber et al., 2012; Harris et al., 2013; Hauri et al., 2013; Turi et al., 2016). The upwelling lasts from spring to early or late fall, when winter storms return. Within the CCLME, the upwelling supports highly productive communities and fisheries on the continental shelf and slope, and in the estuaries (Hickey, 1979; Thomson et al., 1989; Thomson and Krassovski, 2010). Thus, while upwelling plays a defining role in CCLME biogeochemistry, productivity, and ecology, it also contributes to the impacts of local and regional oceanographic processes that exacerbate the effects of anthropogenic OA. Here we use the term “corrosive” to refer to waters that are undersaturated with respect to aragonite ( $\Omega_{\text{ar}} < 1$ ), a condition that results from some combination of: 1) oceanic uptake of anthropogenic  $\text{CO}_2$  and 2) build-up of  $\text{CO}_2$  from the natural respiration processes in the ocean interior ( $C_{\text{bio}}$ ) that occur in offshore waters prior to upwelling or on the continental shelf after those interior waters have upwelled. These processes are already affecting coastal regions such that corrosive waters have previously been observed in large coastal regions including Arctic and Alaskan coastal waters, as well as the CCLME (Feely et al., 2008; Bates et al., 2013; Mathis et al., 2014a,b; 2015).

Many of the ecosystems within the CCLME are particularly vulnerable because of the combined effects of acidification, warming, upwelling, and hypoxia, which are expected to increase under anthropogenic climate change (Rykaczewski and Dunne, 2010; Somero et al., 2016). The term “hypoxia” implies diminished levels of oxygenation under which many species of fish and invertebrates are negatively impacted. Conditions ranging from hypoxic ( $<65 \mu\text{mol kg}^{-1}$ ) to anoxic ( $0 \mu\text{mol kg}^{-1}$ ) have been

observed in near-bottom waters on the inner continental shelf within the CCLME, particularly in the late summer and early fall months when respiration-induced oxygen depletions are at their maximum extent (Grantham et al., 2004; Hales et al., 2006; Chan et al., 2008; Booth et al., 2012; Siedlecki et al., 2016). High  $\text{CO}_2$  concentrations and hypoxia are linked mechanistically because aerobic respiration of organic matter consumes oxygen and produces  $\text{CO}_2$  in approximate stoichiometric equivalence (170:117) (Anderson and Sarmiento, 1994). Thus, processes that create aquatic oxygen deficits can also exacerbate corrosive conditions for calcareous organisms.

## 2. Methodology

### 2.1. Chemical methods

In the late spring of 2007 and late summers of 2011, 2012, and 2013 we conducted detailed observations of carbonate system chemistry and other physical, chemical, and biological parameters along the western North American continental shelf, both via ship-based cruises and shore-based sampling (Fig. 1). Water samples from the cruises were collected in modified Niskin-type bottles and

analyzed under laboratory conditions for dissolved inorganic carbon (DIC), total alkalinity (TA), oxygen, and nutrients. During the cruises in 2011 and 2013, samples were also measured directly for  $\text{pH}_T$ . DIC was analyzed using coulometric titration (Johnson et al., 1987; DOE, 1994; Ono et al., 1998). TA was measured by the potentiometric titration method (Millero et al., 1993; DOE, 1994; Ono et al., 1998). Certified Reference Materials were analyzed with both the DIC and TA samples as an independent verification of instrument calibrations (Dickson et al., 2007). The ship-based DIC and TA data are both precise and accurate to within  $2 \mu\text{mol kg}^{-1}$ . The spectrophotometric method described in Byrne et al. (2010) and Liu et al. (2011) was used to measure pH on the total scale ( $\text{pH}_T$ ) for the 2011 and 2013 cruises. Shore-based measurements of  $\text{pH}_T$  from *in-situ* sensors and DIC and TA from discrete samples were also provided through the OMEGAS (8 sites) and UC Davis Coastal Transect (47 sites) projects, respectively. *In-situ* records were collected using Durafet<sup>®</sup>-based sensors that were calibrated against seawater and/or TRIS-based Certified Reference Materials. Bottle samples were analyzed for DIC (via infrared  $\text{CO}_2$ ; Monterey Bay Aquarium Research Institute) and TA (Metrohm 855 autotitrator), and were cross-verified with pH determined spectrophotometrically for pH, using the total pH scale. The saturation state of

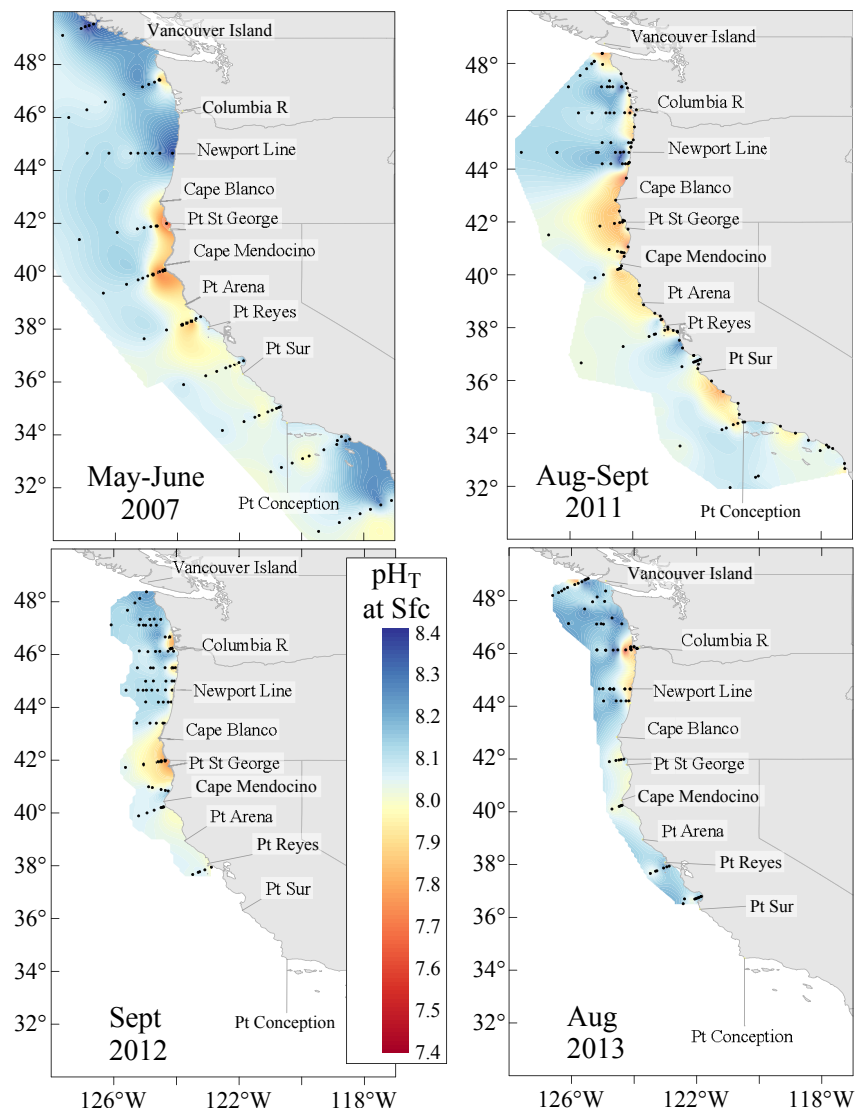
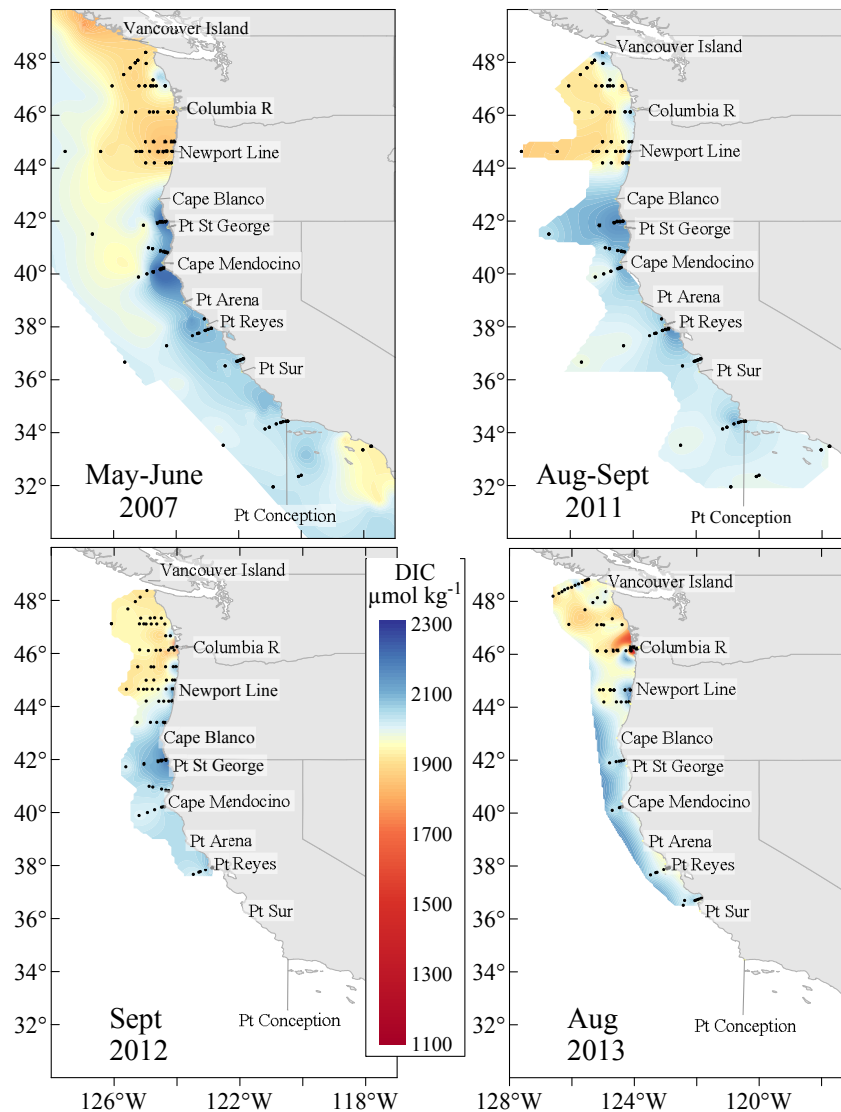


Fig. 2. Maps of surface ocean  $\text{pH}_T$  values for the 2007, 2011, 2012, and 2013 cruises. The 2011 map includes the shore-based intertidal data.



**Fig. 3.** Maps of surface DIC concentrations in  $\mu\text{mol kg}^{-1}$  for the 2007, 2011, 2012, and 2013 cruises. The nearshore upwelling regions are delineated by DIC concentrations in excess of  $2050 \mu\text{mol kg}^{-1}$ . Black dots indicate measurement locations. Open circles on the 2011 and 2013 cruises indicate stations where both chemical and biological samples were taken.

seawater with respect to aragonite was calculated from the DIC and TA data using the program CO2SYS developed by Lewis and Wallace (1998), using the Lueker et al. (2000) carbonate constants, Dickson (1990) for the  $\text{KSO}_4$ , and Lee et al. (2010) for total boron. The pressure effect on the solubility, for samples collected at depth, is estimated from the equation of Mucci (1983), incorporating adjustments to the constants recommended by Millero (1995). Based on the uncertainties in the DIC and TA measurements and the thermodynamic constants, the uncertainty in the calculated  $\Omega_{\text{ar}}$  is approximately 0.02. Oxygen analysis was conducted by modified Winkler titration (Carpenter, 1965), and nutrients (nitrate, nitrite, ammonium, phosphate, silicate) were frozen at sea and analyzed using a Technicon AutoAnalyzer II (UNESCO, 1994) at Oregon State University.

## 2.2. Pteropod shell dissolution

Pteropod shell dissolution was determined on shells collected from 16 stations for the 2011 cruise and 20 stations during the 2013 cruise. The samples were stored in 90% buffered ethanol. Between

15 and 30 pteropods of *Limacina helicina* were blindly picked from samples selected randomly with no prior knowledge of station location or carbonate chemistry conditions. Following the methods described in Bednarek et al. (2012c), the shells were repeatedly washed with distilled water before being subjected to chemical shell dehydration, followed by a plasma etching procedure for periostracum removal. All treated shells were analyzed for shell dissolution using a scanning electron microscope (SEM) and identified for the presence of dissolution patterns and the proportion of more severe types of shell dissolution (Type II and Type III). Following the categorization scheme outlined in Bednarek et al. (2012c), Type II dissolution indicates deeper penetrating dissolution that precedes Type III, which affects large parts of shell crystalline structure, making shells less compact and more fragile.

## 2.3. Estimating coastal $C_{\text{anth}}$ and $C_{\text{bio}}$

Seawater upwelling along the continental shelf of the west coast of North America comes from the thermocline waters of the North Pacific subtropical and subarctic gyres. We therefore used the gyre



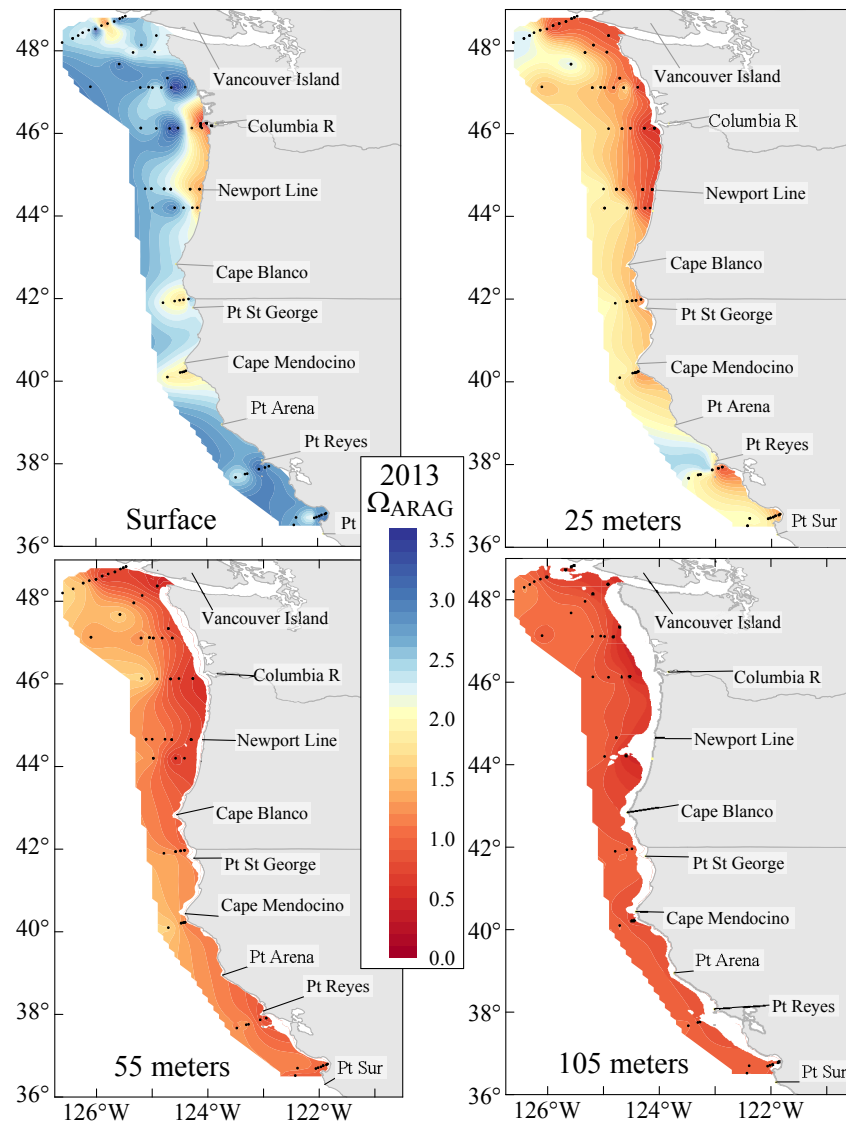


**Figure 4.** Aragonite saturation state at the surface, 25 m, 55 m, and 105 m depth during the 2013 West Coast survey.

thermocline  $C_{\text{anth}}$ , estimated by Carter et al. (submitted) employing the methods outlined in Supplementary Materials section SM1.1 (this paper) -to estimate upwelling water  $C_{\text{anth}}$  for the years 2007, 2011, 2012, and 2013. This method is similar to the approach used by Feely et al. (2008). Our approach for estimating coastal  $C_{\text{anth}}$  and biological remineralization  $C$  ( $C_{\text{bio}}$ ) involves the following steps:

1. Open ocean  $C_{\text{anth}}$  estimates are used to derive polynomials relating thermocline  $C_{\text{anth}}$  to potential density  $\sigma_{\theta}$  for both 2004 and 2013 along P02 (two polynomials) and in 2006 and 2015 along P16N (two additional polynomials). See Supplementary Materials section SM1.2 for details on this step.
2. A grid of seawater properties shoreward of the 200 m depth isobath is determined along the West Coast from our hydrographic surveys in 2007, 2011, 2012, and 2013 using the procedure detailed in the Supplementary Materials section SM1.3.
3. The four polynomials determined in step 1 are used with the  $\sigma_{\theta}$  estimates determined in step 2 to estimate  $C_{\text{anth}}$  for all gridded locations.
4. We interpolate among the four estimates from step 3 to obtain sets of estimates specific to the 4 years of interest (2007, 2011,

2012, and 2013) at each location. We interpolate among the four polynomials both by date to select between the earlier and later polynomials for each section, and by gridded seawater spiciness to select between the P02 and P16 polynomials.

5. We directly estimate  $C_{\text{bio}}$ , or the amount of additional DIC present as a result of organic matter remineralization, from seawater properties using methods described in detail in Supplementary Materials SM1.2.

These gridded properties are used for volume-weighted seawater average properties. Also in SM1.2, the uncertainties in these quantities are estimated to be of order  $\pm (1\sigma) 10 \mu\text{mol kg}^{-1}$ , yielding a 95% confidence interval of  $\sim 20 \mu\text{mol kg}^{-1}$ . We refer to the sum of  $C_{\text{anth}}$  and  $C_{\text{bio}}$  as “enriched DIC.”

### 3. Results

#### 3.1. Coastal distributions of acidified water

During the four cruises, various stages and strengths of upwelling were observed from central Vancouver Island, Canada to

Baja California, Mexico. The observations revealed that, on average, acidified, corrosive  $\text{CO}_2$ -rich waters (*insitu*  $\text{pH}_T < 7.75$ ;  $\Omega_{\text{ar}} < 1.0$ ;  $\text{DIC} > 2190 \mu\text{mol kg}^{-1}$ ) were upwelled from depths of 150–250 m to depths as shallow as 20–200 m in most areas and close to the surface in the region between northern California near Cape Mendocino to Heceta Head, Oregon (Figs. 2–4). Maps of surface ocean  $\text{pH}_T$  and DIC during the four West Coast survey cruises show that *insitu*  $\text{pH}_T$  values ranged from 7.7 to 8.3, with the lowest  $\text{pH}_T$  values and highest DIC concentrations occurring in the upwelled water near the coast (Figs. 2 and 3). Moving offshore,  $\text{pH}_T$  values quickly increase to open-ocean values ranging from 8.0 to 8.3. The 2011  $\text{pH}_T$  map includes complementary shore-based nearshore and intertidal  $\text{pH}_T$  data from the same period, collected using Durafet-style autonomous sensors (Fig. 2), which reinforces the notion that the greatest spatial variability of  $\text{pH}_T$  appears in closest proximity to the shore (Chan et al., submitted). The excellent consistency among the intertidal, nearshore, and offshore data suggests that the uptake of anthropogenic  $\text{CO}_2$ , upwelling/mixing, and respiration processes are the primary drivers of  $\text{pH}_T$  distributions along the coast. Our results for the four cruises follow the seasonal patterns described by Chan et al. (submitted) from field data. Consistent with those results, Turi et al. (2016) found similar patterns in their hindcast biogeochemical model outputs, with higher pH values in the spring and lower pH values in the late summer. One exception is the low  $\text{pH}_T$ , high  $\text{O}_2$ , low  $\Omega_{\text{ar}}$  values in surface waters immediately seaward of the Columbia River Estuary in 2011, 2012, and 2013, which were dominated by the outflow of low salinity, low alkalinity, and high DIC riverine water in the surface layer (Evans et al., 2013).

The corrosive waters along the inner- and mid-shelf regions were due to the combined impacts of anthropogenic  $\text{CO}_2$  uptake and upwelling of respiration-enriched  $\text{CO}_2$  waters along the coast (Figs. 4 and 5). Nearshore upwelled waters were characterized by low-pH seawater ( $\text{pH} < 7.75$ ) with  $\Omega_{\text{ar}}$  values near or below 1.0 and potential density  $> 26.0 \text{ kg m}^{-3}$ . In 2013, for example, along Line 6 offshore of Newport, Oregon, the  $26.1 \text{ kg m}^{-3}$  potential density surface shoaled from a depth range of 150–200 m offshore to the surface near the coast (Fig. 5). This density surface was co-located with isolines of  $\Omega_{\text{ar}} = 1.0$ ,  $\text{DIC} = 2190 \mu\text{mol kg}^{-1}$ , and  $\text{pH} = 7.75$ . However, pH decreased, and DIC and the partial pressure of  $\text{CO}_2$  ( $\text{pCO}_2$ ) increased shoreward in the region surrounding this isopycnal due to  $\text{CO}_2$  release from local remineralization of organic matter. Upwelling of  $\text{CO}_2$ -enriched seawater caused the entire water column shoreward of the 50 m isobath along Line 6 (west of Newport, OR) to become undersaturated with respect to aragonite (Fig 5D). The lowest  $\Omega_{\text{ar}}$  values ( $< 0.70$ ) found shoreward of the 200 m isobath were observed in the near-bottom waters of the mid-shelf region where respiration provides an additional  $\text{CO}_2$  contribution that decreases  $\Omega_{\text{ar}}$ . The uptake of anthropogenic  $\text{CO}_2$  has caused the corrosive ( $\Omega_{\text{ar}} < 1$ ) waters to shoal by about 30–50 m since preindustrial times such that they are within the density layers that are currently being upwelled along the west coast of North America (Feely et al., 2012b).

### 3.2. Pteropod dissolution and water chemistry

The water column hydrographic data were combined with the chemical data for the nearshore and offshore regions and the aragonite saturation state ( $\Omega_{\text{ar}}$ ) was calculated for the upper 55 m or 100 m of the water column in the nearshore and offshore, respectively. Diel vertical migration of *L. helicina* is within this depth range. The values from the region off Southern California were not taken into account, as we did not have pteropod dissolution data for that region. There was a strong negative linear correlation between the percentage of pteropods with Type II and Type III dissolution

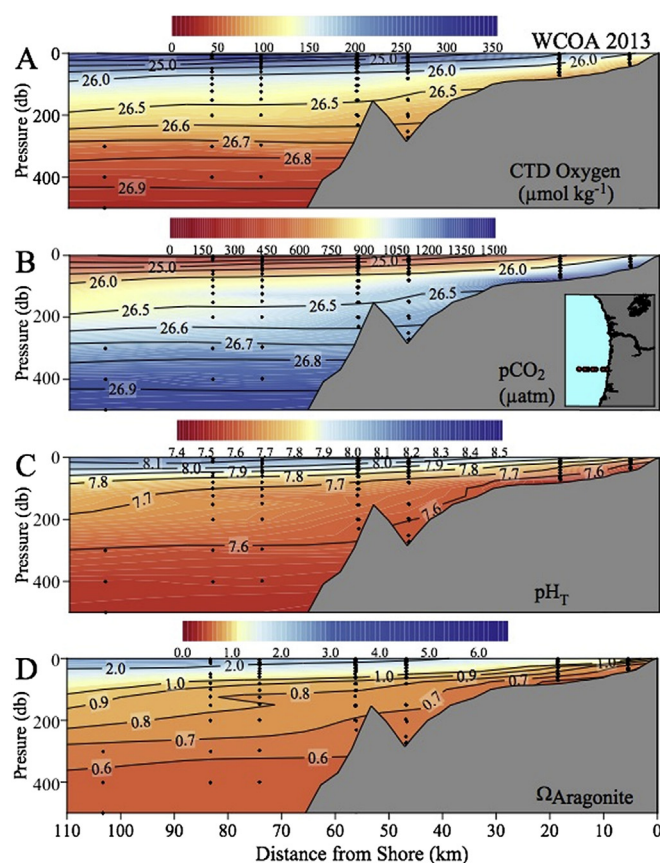


Fig. 5. Vertical sections of: (A) dissolved oxygen, (B)  $\text{pCO}_2$ , (C)  $\text{pH}_T$ , and (D)  $\Omega_{\text{ar}}$  along the 2013 Line 6 stations off Newport, OR. Black dots indicate measurement locations and the isolines in (A) and (B) show the potential density in  $\text{kg m}^{-3}$ .

shell impacts and  $\Omega_{\text{ar}}$  in 2011 and 2013 (Fig. 6,  $R^2 = 0.74$ ,  $p < 0.001$ ). We have fitted the combined data (2011 and 2013) to a logarithmic function and generated the equation:  $y = -66.29 \ln x + 61.21$  ( $R^2 = 0.74$ ). This relationship was used for estimating the

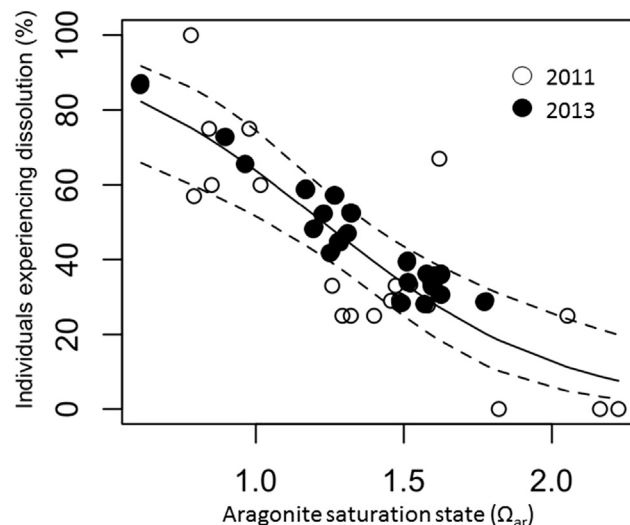


Fig. 6. Percentage of individuals affected by severe dissolution as a function of aragonite saturation state (integrated over the upper 100 m) for the 2011 (open circles) and 2013 (closed circles) data. The dashed lines show the 95% confidence interval for the logarithmic function.

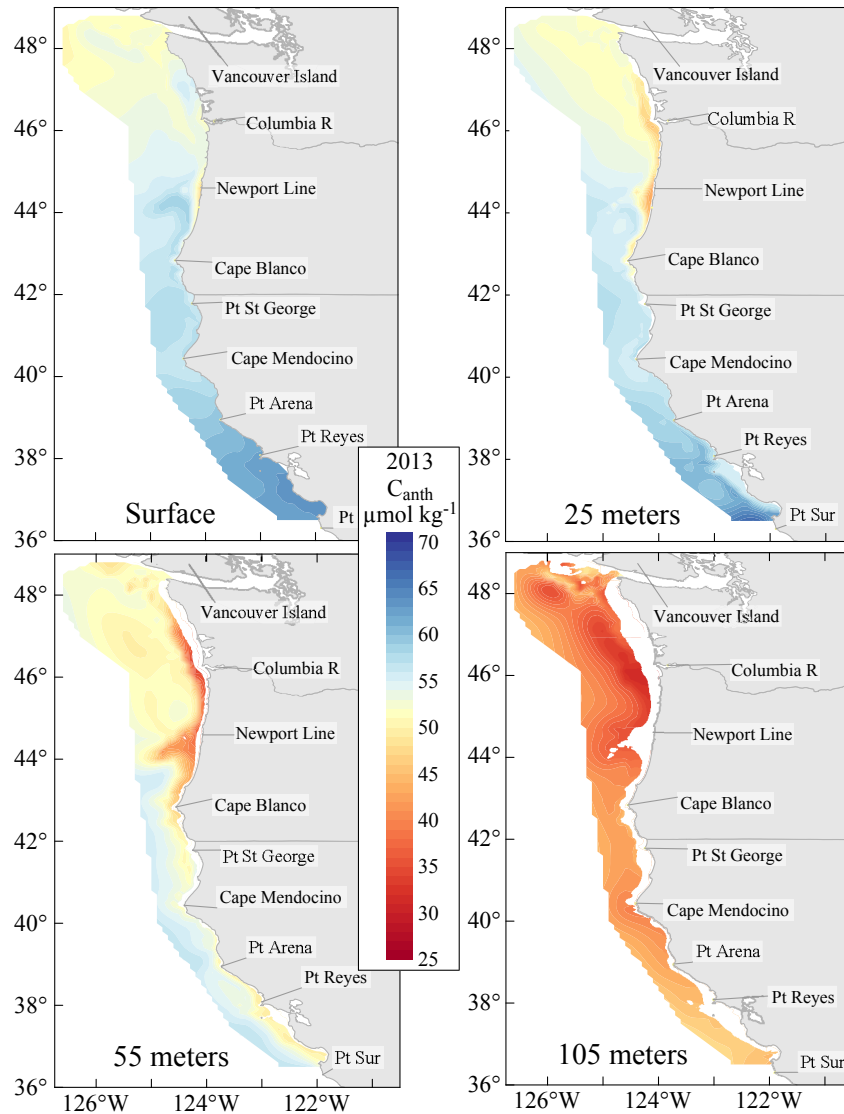
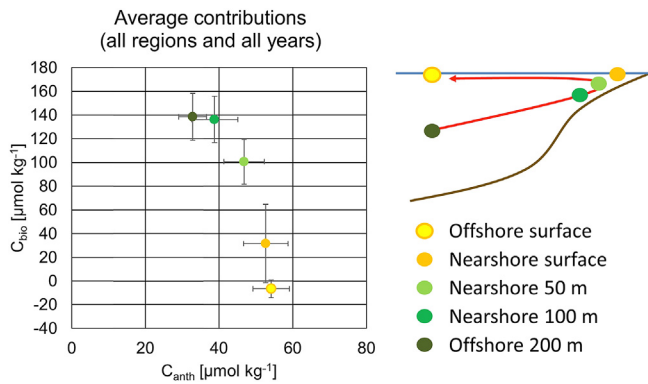


Fig. 7. Distribution of  $C_{anth}$  in  $\mu\text{mol kg}^{-1}$  at the surface, 25 m, 55 m, and 105 m depth for the 2013 West Coast survey.

**Table 1**  
 Anthropogenic carbon ( $C_{anth}$ ), remineralized carbon ( $C_{bio}$ ) and anthropogenic percentage of total enriched carbon ( $\%C_{anth}$ ) by region (W: Washington, O: Oregon, NC: Northern California, SC: Southern California), cruise year, and depth for averages of gridded coastal properties shoreward of the 200 m isobath (left columns) and for the northwestern stations occupied offshore of each region (right columns). All values are expressed in  $\mu\text{mol kg}^{-1}$ . Estimated average uncertainty is approximately  $\pm 10 \mu\text{mol kg}^{-1}$  ( $1\sigma$ ). Column averages are calculated weighting all regions and years equally. Negative  $C_{bio}$  values suggest either net autotrophy or physically derived oxygen supersaturation.

Depths		Grid average shoreward of 200 m isobath									Northwestern station in region					
		0-10 m			50-60 m			100-110 m			Surface			200 m		
State	Year	$C_{anth}$	$C_{bio}$	$\%C_{anth}$	$C_{anth}$	$C_{bio}$	$\%C_{anth}$	$C_{anth}$	$C_{bio}$	$\%C_{anth}$	$C_{anth}$	$C_{bio}$	$\%C_{anth}$	$C_{anth}$	$C_{bio}$	$\%C_{anth}$
W	2007	47	-27	232	47	85	35	34	131	21	47	-5	113	30	140	18
W	2011	51	97	34	47	125	27	36	149	20	54	0	101	33	133	20
W	2012	52	83	39	49	117	29	36	150	19	55	-7	114	30	154	16
W	2013	53	48	53	48	111	30	39	153	20	55	-6	113	31	159	16
O	2007	47	24	66	44	93	32	34	147	19	48	-9	122	32	117	21
O	2011	52	31	62	42	114	27	34	158	18	52	-5	112	35	99	26
O	2012	54	18	75	48	88	35	39	131	23	53	-1	102	33	143	19
O	2013	55	37	60	46	121	27	37	149	20	56	-7	115	33	141	19
NC	2007	37	32	54	33	96	26	29	135	18	44	-10	128	27	134	17
NC	2011	57	49	54	47	108	30	42	138	23	56	-5	110	27	157	15
NC	2012	58	28	68	53	82	39	49	112	30	56	4	94	33	140	19
NC	2013	60	17	78	52	97	35	43	137	24	58	-8	115	33	139	19
SC	2007	55	-22	167	43	116	27	38	135	22	51	-6	114	32	153	17
SC	2011	59	28	68	56	56	50	53	82	39	58	0	99	42	95	31
SC	2012	-	-	-	-	-	-	-	-	-	60	-9	117	37	155	19
SC	2013	-	-	-	-	-	-	-	-	-	63	-31	196	37	157	19
Averages		53	28	65	47	102	32	39	136	22	54	-7	115	33	139	19



**Figure 8.** Plot of  $C_{bio}$  vs  $C_{anth}$  in offshore and nearshore waters in the California Current Large Marine Ecosystem. The simple schematic in the upper right is a cross section of the coast with offshore being to the left, and with the mean path of upwelling water indicated as a red arrow. Error bars express standard deviations for various estimates from each region and depth (Table 1) rather than uncertainty, which is approximately  $\pm 10 \mu\text{mol kg}^{-1}$  ( $1\sigma$ ) for  $C_{bio}$  and  $C_{anth}$ .

percentage of individuals with severe dissolution for both pre-industrial and current  $\Omega_{ar}$  values (Table 2).

During both 2011 and 2013 cruises, pteropod shell dissolution was observed to be significantly higher in the nearshore region of the CCLME. Currently, on average 57% of individuals are affected by dissolution in the nearshore regions, but only 36% in the offshore region (Table 2). This greater incidence of dissolution-affected individuals is consistent with lower aragonite saturation state in the nearshore region (average  $\Omega_{ar} = 1.07$ ) compared to the offshore region (average  $\Omega_{ar} = 1.47$ ).

## 4. Discussion

### 4.1. Estimates of $C_{anth}$ and $C_{bio}$ in the CCLME

Because the increased DIC concentrations along the coast are the result of uptake of  $C_{anth}$  and upwelling of  $\text{CO}_2$ -rich respired  $\text{CO}_2$  ( $C_{bio}$ ) waters from below we have estimated the contributions of both  $C_{anth}$  and  $C_{bio}$  throughout the water column. Our estimates of the distribution of  $C_{anth}$  from the coast out to the open-ocean for 2013 are presented as maps for surface, 25, 55, and 105 m (Fig. 7), and a summary of the regional averages are given in Table 1. In nearshore surface waters,  $C_{anth}$  ranges from about 37 to  $60 \mu\text{mol kg}^{-1}$ , with increasing concentrations north and south of the region near Cape Blanco. The lowest  $C_{anth}$  concentrations (ranging from 37 to  $55 \mu\text{mol kg}^{-1}$ ) are centered near the strong upwelling center between the region south of the Columbia River to Cape Mendocino. To the north and south of this region nearshore  $C_{anth}$  concentrations are somewhat higher, indicating mixing of the upwelled water with water that has been in recent contact with the atmosphere. The highest  $C_{anth}$  concentrations (ranging from 44 to  $63 \mu\text{mol kg}^{-1}$ ) are located in the offshore surface waters. At 25 m in the nearshore region, the influence of the upwelled water is more pronounced, with  $C_{anth}$  concentrations ranging from 33 to

$55 \mu\text{mol kg}^{-1}$  along most of the coastline. At deeper nearshore depths,  $C_{anth}$  ranges from 33 to  $56 \mu\text{mol kg}^{-1}$  at 55 m and from 29 to  $53 \mu\text{mol kg}^{-1}$  at 105 m.

Average  $C_{anth}$  and  $C_{bio}$  concentrations are shown in Fig. 8 and a summary of the regional and depth averages for  $C_{anth}$  and  $C_{bio}$  is given in Table 1. For comparison, Table 1 shows enriched carbon contributions found at the surface and at 200 m depth at the most northwestern station (i.e., most offshore) within each study region. In offshore surface waters, nearly all of the enriched DIC ( $C_{anth} + C_{bio}$ ) is from  $C_{anth}$ , whereas at 200 m only about 19% of the enriched DIC is from  $C_{anth}$  and the remainder is from  $C_{bio}$ .

In the nearshore region of the CCLME, enriched DIC in surface waters ranged from 41 to  $148 \mu\text{mol kg}^{-1}$ , with an average of about 65% of enriched DIC in the surface waters due to  $C_{anth}$  and the remainder due to  $C_{bio}$ . Enriched DIC at 50 m is larger than at the surface (range: 129– $172 \mu\text{mol kg}^{-1}$ ), but the percentage due to  $C_{anth}$  is lower (~32%). Finally, at 100 m, only about 22% of the enriched DIC is due to  $C_{anth}$ . There is some year-to-year variability within the regions but the highest contributions of  $C_{anth}$  and total enriched-DIC generally occur in the later years. While the percentage of  $C_{anth}$  in the nearshore upwelled water is lower than the surrounding water, the total amount of enriched DIC is highest in the nearshore upwelled water and, consequently, those nearshore upwelled waters are the most corrosive to calcifying organisms. In subsurface waters, the most corrosive conditions occur in the onshore bottom waters within 20 km of the coast. The uptake of  $C_{anth}$  has caused the aragonite saturation horizon to shoal by approximately 30–50 m since the preindustrial period so that undersaturated waters are well within the regions of the continental shelf that affect the shell dissolution of living pteropods (Feely et al., 2008).

### 4.2. Biological impacts evaluated as pteropod shell dissolution

Co-locating biological responses and chemical observations allows for direct comparison of results in 2011 and 2013. Pteropod dissolution has been found to be highly correlated with aragonite saturation conditions in 2011 (Bednarek et al., 2014a). Consequently, we have used the same procedure to also correlate the extent of dissolution also for 2013. Pteropod shell dissolution significantly increased from offshore to nearshore in the CCLME. Pteropods were ~22% more likely to be affected by severe shell dissolution in nearshore waters compared with offshore waters. Consistent with these results, nearshore  $\Omega_{ar}$  values were approximately 40% lower than offshore values, indicating a strong negative correlation between the percentage of pteropod individuals with severe shell dissolution and  $\Omega_{ar}$  (Fig. 6).

In 2011 and 2013,  $C_{anth}$  contributed approximately 22–65% of the enriched DIC in the coastal areas over the period of the spring and summer measurements through the top 100 m (Table 1). This contribution lowered average seawater  $\Omega_{ar}$  values from approximately 1.39 to 1.05 in the nearshore region in 2011, and from 1.46 to 1.08 in 2013. Offshore, the contribution of  $C_{anth}$  reduced  $\Omega_{ar}$  from an average of 2.21 to 1.51 in 2011, and from 2.09 to 1.43 in 2013 since the pre-industrial times. Consequently, based on the newly

**Table 2**

Average pre-industrial and current aragonite saturation states (calculated for years 2011 and 2013) and average percentage of individuals affected by severe dissolution in the pre-industrial times and currently for the nearshore and offshore regions of CCLME.

Year	Location	$\Omega_{ar}$ , preind.	$\Omega_{ar}$ , current	% Ind. with severe dissolution, preind.	% Ind. with severe dissolution, current
2011	nearshore	1.39	1.05	39	58
2013	nearshore	1.46	1.08	36	56
2011	offshore	2.21	1.51	8	34
2013	offshore	2.09	1.43	12	37



developed relationships in Fig. 6, we estimate that the percentage of pteropods affected with severe dissolution due to the Canth contribution in 2011 increased 19% in the nearshore waters and 26% in the offshore waters (Table 2). In 2013, we estimate Canth had increased the percentage of individuals affected by dissolution by 20% and 25% in nearshore and offshore waters, respectively (Table 2). The 2013 results are comparable to the results for 2011, providing further evidence for increasing incidence of severe dissolution with increasing Canth and decreasing  $\Omega_{ar}$ . The estimate of pteropod dissolution from Canth is comparable to that reported previously (Bednaršek et al., 2014a), where dissolution was estimated based on the difference between pre-industrial and current DIC values.

The observed relationship between  $\Omega_{ar}$  and severe shell dissolution suggests that changes in the carbonate chemistry due to Canth are already having an impact on *L. helicina*. Although the percentage of individuals affected by dissolution in the nearshore region is ~22% greater than in the offshore region, the increase due to anthropogenic CO<sub>2</sub> of approximately 19–26% is comparable in both regions. Surprisingly, the relative change in the extent of pteropod dissolution in the offshore regions suggest that they are at least as vulnerable, or perhaps even more vulnerable, to the changes imposed by the Canth uptake over the last several decades. This may be related to the much lower natural variability in offshore waters as compared with the nearshore waters.

Shell dissolution as observed in pteropods along the west coast of North America affects their swimming abilities (Bednaršek et al., unpublished results), and can potentially enhance predation pressure and increase energetic costs of vital biological processes (Lischka et al., 2011; Wood et al., 2008; Manno et al., 2012). This chronic exposure to undersaturated conditions results in sub-lethal effects of compromised physiological state that may, over longer time periods, affect the overall pteropod population in the CCLME (Weisberg et al., 2016). Given that pteropods are equally abundant nearshore and offshore (Mackas and Galbraith, 2012; Bednaršek et al., 2012b), changes due to OA intensification might have ecological implications in both regions. Additionally, the role of pteropods as potentially important prey species requires better understanding of trophic interactions with their predators on the regional level in the CCLME. Integrating pteropods as an independent functional group in end-to-end modeling efforts can help reveal the impacts of potential pteropod biomass decreases on higher trophic levels. Introducing pteropods in such models would require incorporating information on pteropod diet, life-history stages, and physiological and feeding responses, which has recently been reviewed by Bednaršek et al. (2016).

## 5. Conclusions

By combining chemical and biological studies in the field we are able to provide a clearer picture of the extent of  $C_{anth}$  distributions and its likely impact on pteropod shell dissolution. Our results suggest that large-scale declines in the aragonite saturation states of the CCLME resulting from the uptake of  $C_{anth}$  in open-ocean and coastal waters are leading to increased incidence of pteropod shell dissolution and potentially creating significant challenges for these organisms. Since the pre-industrial times, pteropod shell dissolution has, on average, increased approximately 19–26% in both nearshore and offshore waters in the CCLME. The capacity of these organisms to acclimatize and adapt to OA, amid concurrent changes in temperature, dissolved oxygen, and other drivers remains largely unknown. Nevertheless, the results shown here clearly indicate that humankind may already be having a significant impact on a species that may play a vital role in this large and important marine ecosystem.

## Acknowledgments

The National Oceanic and Atmospheric Administration (NOAA) (Grant No. OAPFY2014.03.PMEL.003) and the National Science Foundation (Grant No. OCE 1041240) sponsored this work. We specifically thank Libby Jewett and Dwight Gledhill of the NOAA Ocean Acidification Program, Kenneth Mooney and Kathy Tedesco of the NOAA Climate Program, and Dave Garrison of the National Science Foundation for their support. Nina Bednaršek was supported by the NOAA Pacific Marine Environmental Laboratory (Grant No. OAPFY2014.03.PMEL.003), the Educational Foundation of America, and the Washington Ocean Acidification Center. This is PMEL contribution number 4355.

## Appendix A. Supplementary data

Supplementary data related to this article can be found at <http://dx.doi.org/10.1016/j.ecss.2016.08.043>.

## References

- Anderson, L.A., Sarmiento, J.L., 1994. Redfield ratios of remineralization determined by nutrient data analysis. *Glob. Biogeochem. Cy.* 8 (1), 65–80. <http://dx.doi.org/10.1029/93GB03318>.
- Armstrong, J.L., Boldt, J.L., Cross, A.D., Moss, J.H., Davis, N.D., Myers, K.W., Walker, R.V., Beauchamp, D.A., Halderson, L.J., 2005. Distribution, size, and interannual, seasonal and diel food habits of northern Gulf of Alaska juvenile pink salmon, *Oncorhynchus gorbuscha*. *Deep Sea Res. Part II* 52, 247–265.
- Aydin, K.Y., McFarlane, G.A., King, J.R., Megrey, B.A., Myers, K.W., 2005. Linking oceanic food webs to coastal production and growth rates of Pacific salmon (*Oncorhynchus* spp.), using models on three scales. *Deep Sea Res. Part II* 52, 757–780.
- Barton, A., Hales, B., Waldbusser, G., Langdon, C., Feely, R.A., 2012. The Pacific oyster, *Crassostrea gigas*, shows negative correlation to naturally elevated carbon dioxide levels: implications for near-term ocean acidification impacts. *Limnol. Oceanogr.* 57, 698–710. <http://dx.doi.org/10.4319/lo.2012.57.3.0698>.
- Barton, A., Waldbusser, G.G., Feely, R.A., Weisberg, S.B., Newton, J.A., Hales, B., Cudd, S., Eudeline, B., Langdon, C.J., Jefferds, I., King, T., Suhrbier, A., McLaughlin, K., 2015. Impacts of coastal acidification on the Pacific Northwest shellfish industry and adaptation strategies implemented in response. *Oceanography* 28 (2), 146–159. <http://dx.doi.org/10.5670/oceanog.2015.38>.
- Bates, N.R., Orchowaska, M.L., Garley, R., Mathis, J.T., 2013. Summertime calcium carbonate undersaturation in shelf waters of the western Arctic Ocean—how biological processes exacerbate the impact of ocean acidification. *Biogeochemistry* 10, 5281–5309. <http://dx.doi.org/10.5194/bg-10-5281-2013>.
- Bednaršek, N., Tarling, G.A., Bakker, D.C.E., Fielding, S., Jones, E.M., Venables, H.J., Ward, P., Kuzirian, A., Lézé, B., Feely, R.A., Murphy, E.J., 2012a. Extensive dissolution of live pteropods in the Southern Ocean. *Nat. Geosci.* 5, 881–885. <http://dx.doi.org/10.1038/ngeo1635>.
- Bednaršek, N., Možina, J., Vogt, M., O'Brien, C., Tarling, G.A., 2012b. The global distribution of pteropods and their contribution to carbonate and carbon biomass in the modern ocean. *Earth Syst. Sci. Data* 4 (1), 167–186.
- Bednaršek, N., Tarling, G.A., Bakker, D.C., Fielding, S., Cohen, A., Kuzirian, A., Montagna, R., 2012c. Description and quantification of pteropod shell dissolution: a sensitive bioindicator of ocean acidification. *Glob. Change Biol.* 18 (7), 2378–2388.
- Bednaršek, N., Feely, R.A., Reum, J.C.P., Peterson, W., Menkel, J., Alin, S.R., Hales, B., 2014a. *Limacina helicina* shell dissolution as an indicator of declining habitat suitability due to ocean acidification in the California Current Ecosystem. *Proc. Roy. Soc. B* 281, 20140123. <http://dx.doi.org/10.1098/rspb.2014.0123>.
- Bednaršek, N., Tarling, G.A., Bakker, D.C.E., Fielding, S., Feely, R.A., 2014b. Dissolution dominating calcification process in polar pteropods close to the point of aragonite undersaturation. *PLoS One* 9 (10), e109183. <http://dx.doi.org/10.1371/journal.pone.0109183>.
- Bednaršek, N., Harvey, C.J., Kaplan, I.C., Feely, R.A., Možina, J., 2016. Pteropods on the edge: cumulative effects of ocean acidification, warming, and deoxygenation. *Prog. Oceanogr.* 145, 1–24.
- Booth, A.T., McPhee, E.E., Chua, P., Kingsley, E., Denny, M., Phillips, R., Bograd, S.J., Zeidberg, L.D., Gilly, W.F., 2012. Natural intrusions of hypoxic, low pH water into nearshore marine environments on the California coast. *Cont. Shelf Res.* 45, 108–115.
- Byrne, R.H., Mecking, S., Feely, R.A., Liu, X., 2010. Direct observations of basin-wide acidification of the north Pacific Ocean. *Geophys. Res. Lett.* 37, L02601. <http://dx.doi.org/10.1029/2009GL040999>.
- Canadell, J.G., Le Quéré, C., Raupach, M.R., Field, C.B., Buitenhuis, E.T., Ciais, P., Conway, T.J., Houghton, R.A., Marland, G., 2007. Contributions to accelerating atmospheric CO<sub>2</sub> growth from economic activity, carbon intensity, and efficiency of natural sinks. *Proc. Natl. Acad. Sci. U. S. A.* 104 (47), 18866–18870.

- <http://dx.doi.org/10.1073/pnas.0702737104>.
- Carpenter, J.H., 1965. The Chesapeake Bay Institute technique for the Winkler dissolved oxygen method. *Limnol. Oceanogr.* 10 (1), 141–143. <http://dx.doi.org/10.4319/lo.1965.10.1.0141>.
- Carter, B.R., Feely, R.A., Mecking, S., Cross, J.N., Macdonald, A.M., Siedlecki, S.A., Talley, L.D., Sabine, C.L., Millero, F.J., Swift, J.H., Dickson, A.G., 2016. Two decades of Pacific anthropogenic carbon storage and ocean acidification along GO-SHIP sections P16 and P02. *Glob. Biogeochem. Cy.* (in revision).
- Chan, F., Barth, J.A., Lubchenco, J., Kirincich, A., Weeks, H., Peterson, W.T., Menge, B.A., 2008. Emergence of anoxia in the California current large marine ecosystem. *Science* 319 (5865), 920. <http://dx.doi.org/10.1126/science.1149016>.
- Chan, F., Barth, J.A., Blanchette, C.A., Byrne, R.H., Chavez, F., Cheriton, S.O., Feely, R.A., Friedrich, G., Gaylord, B., Gouhier, T., Hacker, S., Hill, T., Hofmann, G., McManus, M.A., Menge, B., Nielsen, K.J., Russell, A., Sanford, E., Sevadjan, J., Washburn, L., 2016. Evidence for widespread progression of nearshore ocean acidification in the California Current System. *Sci. Rep.* (in revision).
- Dickson, A.G., 1990. Thermodynamics of the dissociation of boric acid in synthetic seawater from 273.15 to 298.25 K. *Deep Sea Res.* 37, 755–766.
- Dickson, A.G., Sabine, C.L., Christian, J.R. (Eds.), 2007. *Guide to Best Practices for Ocean CO<sub>2</sub> Measurements*, vol. 3. PICES Special Publication, 191pp.
- DOE, 1994. *Handbook of Methods for the Analysis of the Various Parameters of the Carbon Dioxide System in Sea Water (Version 2)*, ORNL/CDIAC-74.
- Doney, S.C., Balch, W.M., Fabry, V.J., Feely, R.A., 2009a. Ocean acidification: a critical emerging problem for the ocean sciences. *Oceanography* 22 (4), 18–27. <http://dx.doi.org/10.5670/oceanog.2009.93>.
- Doney, S.C., Fabry, V.J., Feely, R.A., Kleypas, J.A., 2009b. Ocean acidification: the other CO<sub>2</sub> problem. *Annu. Rev. Mar. Sci.* 1, 169–192.
- Ekstrom, J.A., Suatoni, L., Cooley, S.R., Pendleton, L.H., Waldbusser, G.G., Cinner, J.E., Ritter, J., Langdon, C., van Hooijdonk, R., Gledhill, D., Wellman, K., Beck, M.W., Brander, L.M., Rittschof, D., Doherty, C., Edwards, P.E.T., Portela, R., 2015. Vulnerability and adaptation of US shellfisheries to ocean acidification. *Nat. Clim. Change* 5, 207–214. <http://dx.doi.org/10.1038/NCLIMATE2508>.
- Evans, W., Hales, B., Strutton, P.G., 2013. pCO<sub>2</sub> distributions and air-water CO<sub>2</sub> fluxes in the Columbia River estuary. *Estuar. Coast. Shelf Sci.* 117, 260–272. <http://dx.doi.org/10.1016/j.ecss.2012.12.003>.
- Fabry, V.J., Seibel, B.A., Feely, R.A., Orr, J.C., 2008. Impacts of ocean acidification on marine fauna and ecosystem processes. *ICES J. Mar. Sci.* 65, 414–432.
- Feely, R.A., Sabine, C.L., Lee, K., Berelson, W., Kleypas, J., Fabry, V.J., Millero, F.J., 2004. Impact of anthropogenic CO<sub>2</sub> on the CaCO<sub>3</sub> system in the oceans. *Science* 305 (5682), 362–366. <http://dx.doi.org/10.1126/science.1097329>.
- Feely, R.A., Sabine, C.L., Hernandez-Ayon, J.M., Ianson, D., Hales, B., 2008. Evidence for upwelling of corrosive “acidified” water onto the Continental Shelf. *Science* 320 (5882), 1490–1492. <http://dx.doi.org/10.1126/science.1155676>.
- Feely, R.A., Doney, S.C., Cooley, S.R., 2009. Ocean acidification: present conditions and future changes in a high-CO<sub>2</sub> world. *Oceanography* 22 (4), 36–47. <http://dx.doi.org/10.5670/oceanog.2009.95>.
- Feely, R.A., Sabine, C.L., Byrne, R.H., Millero, F.J., Dickson, A.G., Wanninkhof, R., Murata, A., Miller, L.A., Greeley, D., 2012a. Decadal changes in the aragonite and calcite saturation state of the Pacific Ocean. *Glob. Biogeochem. Cy.* 26, GB3001. <http://dx.doi.org/10.1029/2011GB004157>.
- Feely, R.A., Klinger, T., Newton, J.A., Chadsey, M., 2012b. *Scientific Summary of Ocean Acidification in Washington State Marine Waters*. NOAA OAR Special Report, 170 pp.
- Frieder, C.A., Gonzalez, J.P., Bockmon, E.E., Navarro, M.O., Levin, L.A., 2014. Can variable pH and low oxygen moderate ocean acidification outcomes for mussel larvae? *Glob. Change Biol.* 20, 754–764.
- Gattuso, J.-P., Hansson, L., 2011. Ocean acidification: background and history. In: Gattuso, J.-P., Hansson, L. (Eds.), *Ocean Acidification*. Oxford Univ. Press, Oxford, pp. 1–20.
- Gattuso, J.-P., Magnan, A., Bille, R., Cheung, W.W.L., Howes, E.L., Joos, F., Allemand, D., Bopp, L., Cooley, S.R., Eakin, C.M., Hoegh-Guldberg, O., Kelly, R.P., Pörtner, H.-O., Rogers, A.D., Baxter, J.M., Laffoley, D., Osborn, D., Rankovic, A., Rochette, J., Sumaila, U.R., Treyer, S., Turley, C., 2015. Contrasting futures for ocean and society from different anthropogenic CO<sub>2</sub> emission scenarios. *Science* 349 (6243), aac4722. <http://dx.doi.org/10.1126/science.aac4722>.
- Gaylord, B., Hill, T.M., Sanford, E., Lenz, E.A., Jacobs, L.A., Sato, K.N., Russell, A.D., Hettinger, A., 2011. Functional impacts of ocean acidification in an ecologically critical foundation species. *J. Exp. Biol.* 214, 2586–2594.
- Gaylord, B., Kroeker, K.J., Sunday, J.M., Anderson, K.M., Barry, J.P., Brown, N.E., Connell, S.D., Dupont, S., Fabricius, K.E., Hall-Spencer, J.M., Klinger, T., Milazzo, M., Munday, P.L., Russell, B.D., Sanford, E., Schreiber, S.J., Thiyagarajan, V., Vaughan, M.L.H., Widdicombe, S., Harley, C.D.G., 2015. Ocean acidification through the lens of ecological theory. *Ecology* 96, 3–15.
- Grantham, B.A., Chan, F., Nielsen, K.J., Fox, D.S., Barth, J.A., Lubchenco, J., Menge, B.A., 2004. Upwelling-driven nearshore hypoxia signals ecosystem and oceanographic changes in the northeast Pacific. *Nature* 429 (6993), 749–754. <http://dx.doi.org/10.1038/nature02605>.
- Groot, C., Margolis, L. (Eds.), 1991. *Pacific Salmon Life Histories*. UBC Press, Vancouver, Canada.
- Gruber, N., Hauri, C., Lachkar, Z., Loher, D., Frölicher, T.L., Plattner, G.-K., 2012. Rapid progression of ocean acidification in the California Current System. *Science* 337 (6091), 220–223.
- Guinotte, J.M., Fabry, V.J., 2008. Ocean acidification and its potential effects on marine ecosystems. *Ann. N. Y. Acad. Sci.* 1134, 320–342. <http://dx.doi.org/10.1196/annals.1439.013>.
- Hales, B., Karp-Boss, L., Perlin, A., Wheeler, P., 2006. Oxygen production and carbon sequestration in an upwelling coastal margin. *Glob. Biogeochem. Cy.* 20, GB3001. <http://dx.doi.org/10.1029/2005GB002517>.
- Harris, K.E., DeGrandpre, M.D., Hales, B., 2013. Aragonite saturation state dynamics in a coastal upwelling zone. *Geophys. Res. Lett.* 40, 2720–2725. <http://dx.doi.org/10.1002/grl.50460>.
- Hauri, C., Gruber, N., Vogt, M., Doney, S.C., Feely, R.A., Lachkar, Z., Leinweber, A., McDonnell, A.M.P., Munnich, M., Plattner, G.-K., 2013. Spatiotemporal variability and long-term trends of ocean acidification in the California Current System. *Biogeosciences* 10, 193–216. <http://dx.doi.org/10.5194/bg-10-193-2013>.
- IPCC, 2013. *Climate Change 2013: The Physical Science Basis. Contribution of Working Group I to the Fifth Assessment Report of the Intergovernmental Panel on Climate Change*. Stocker, T.F., Qin, D., Plattner, G.-K., Tignor, M., Allen, S.K., Boschung, J., Nauels, A., Xia, Y., Bex, V., Midgley, P.M. (Eds.). Cambridge University Press, Cambridge, UK and New York, NY, 1535 pp.
- Johnson, K.M., King, A.E., Sieburth, J.M., 1985. Coulometric TCO<sub>2</sub> analyses for marine studies; an introduction. *Mar. Chem.* 16, 61–82.
- Hettinger, A., Sanford, E., Hill, T.M., Russell, A.D., Sato, K.N., Hoey, J., Forsch, M., Page, H.N., Gaylord, B., 2012. Persistent carry-over effects of planktonic exposure to ocean acidification in the Olympia oyster. *Ecology* 93, 2758–2768.
- Hickey, B.M., 1979. The California Current system – hypotheses and facts. *Prog. Oceanogr.* 8, 191–279. [http://dx.doi.org/10.1016/0079-6611\(79\)90002-8](http://dx.doi.org/10.1016/0079-6611(79)90002-8).
- Hofmann, G.E., Todgham, A.E., 2010. Living in the now: physiological mechanisms to tolerate a rapidly changing environment. *Annu. Rev. Mar. Physiol.* 72, 127–145.
- IPCC, 2013. In: Stocker, T.F., Qin, D., Plattner, G.-K., Tignor, M., Allen, S.K., Boschung, J., Nauels, A., Xia, Y., Bex, V., Midgley, P.M. (Eds.), *Climate Change 2013: The Physical Science Basis. Contributions of Working Group I to the Fifth Assessment Report of the Intergovernmental Panel on Climate Change*. Cambridge University Press, Cambridge, United Kingdom and NY, USA, 1535 pp.
- Johnson, K.M., Sieburth, J.M., Williams, P.J.L., Brändström, L., 1987. Coulometric total carbon dioxide analysis for marine studies: automation and calibration. *Mar. Chem.* 21, 117–133.
- Kroeker, K.J., Kordas, R.L., Crim, R., Hendriks, I.E., Ramajo, L., Singh, G.S., Duarte, C.M., Gattuso, J.-P., 2013. Impacts of ocean acidification on marine organisms: quantifying sensitivities and interaction with warming. *Glob. Change Biol.* 19, 1884–1896. <http://dx.doi.org/10.1111/gcb.12179>.
- Lee, K., Kim, T.-W., Byrne, R.H., Millero, F.J., Feely, R.A., Liu, Y.-M., 2010. The universal ratio of boron to chlorinity for the North Pacific and North Atlantic oceans. *Geochim. Cosmochim. Acta* 74 (6), 1801–1811. <http://dx.doi.org/10.1016/j.gca.2009.12.027>.
- Le Quéré, C., Moriarty, R., Andrew, R.M., Canadell, J.G., Sitch, S., Korsbakken, J.L., Peters, G.P., Arntjes, R.J., Boden, T.A., Friedlingstein, P., Houghton, R.A., House, J.I., Keeling, R.F., Marland, G., Tans, P., Arneeth, A., Bakker, D.C.E., Barbero, L., Bopp, L., Chang, J., Chevallier, F., Chini, L.P., Ciais, P., Fader, M., Feely, R.A., Gkritzalis, T., Harris, I., Hauck, J., Ilyana, T., Jain, A.K., Kato, E., Kitidis, V., Klein Goldewitz, K., Koven, C., Landschützer, P., Lavusset, S.K., Lefèvre, N., Lenton, A., Lima, I.D., Metz, N., Millero, F., Munro, D., Murata, A., Nabel, J.E.M.S., Nakaoka, S., Nojiri, Y., O'Brien, K., Olsen, A., Ono, T., Pérez, F.F., Pfeil, B., Pierrot, D., Poulter, B., Rehder, G., Rödenbeck, C., Saito, S., Schuster, U., Schwinger, J., Séférian, R., Steinhoff, T., Stocker, B.D., Sutton, A.J., Takahashi, T., Tilbrook, B., van der Laan-Luijckx, I., van der Werf, G.R., van Heuven, S., Vandemark, D., Viovy, N., Wiltshire, A., Zaehle, S., 2015. Global carbon budget 2015. *Earth Sys. Sci. Data* 7, 349–396. <http://dx.doi.org/10.5194/essd-7-349-2015>.
- Lewis, E., Wallace, D.W.R., 1998. Program Developed for CO<sub>2</sub> System Calculations. ORNL/CDIAC-105. Carbon Dioxide Information Analysis Center. Oak Ridge National Laboratory, Oak Ridge, Tenn. Available online at: [http://cdiac.ornl.gov/ftp/co2sys/CO2SYS\\_calc\\_DOS\\_v1.05/cdiac105.pdf](http://cdiac.ornl.gov/ftp/co2sys/CO2SYS_calc_DOS_v1.05/cdiac105.pdf).
- Lischka, S., Buedenbender, J., Boxhammer, T., Riebesell, U., 2011. Impact of ocean acidification and elevated temperatures on early juveniles of the polar shelled pteropod *Limacina helicina*: mortality, shell degradation, and shell growth. *Biogeosciences* 8, 919–932.
- Liu, X., Patsavas, M.C., Byrne, R.H., 2011. Purification and characterization of meta-cresol purple for spectrophotometric seawater pH measurements. *Environ. Sci. Technol.* 45 (11), 4862–4868.
- Lueker, T.J., Dickson, A.G., Keeling, C.D., 2000. Ocean pCO<sub>2</sub> calculated from dissolved inorganic carbon, alkalinity, and equations for K<sub>1</sub> and K<sub>2</sub>: validation based on laboratory measurements of CO<sub>2</sub> in gas and seawater at equilibrium. *Mar. Chem.* 70 (1–3), 105–119.
- Mackas, D.L., Galbraith, M.D., 2012. Pteropod time-series from the NE Pacific. *ICES J. Mar. Sci.* 69 (3), 448–459. <http://dx.doi.org/10.1093/icesjms/fsr163>.
- Manno, C., Morata, N., Primicerio, R., 2012. *Limacina retroversata* response to combined effects of ocean acidification and sea water freshening. *Estuar. Coast. Shelf Sci.* 113, 163–171.
- Mathis, J.T., Cross, J.N., Monacci, N., Feely, R.A., Stabeno, P.J., 2014a. Evidence of prolonged aragonite undersaturations in the bottom waters of the southern Bering Sea shelf from autonomous sensors. *Deep Sea Res. II* 109, 125–133. <http://dx.doi.org/10.1016/j.dsr2.2013.07.019>.
- Mathis, J.T., Grebeiner, J.G., Hansell, D.A., Hopcroft, R.R., Kirchman, D.L., Lee, S.H., Moran, S.B., Bates, N.R., VanLaningham, S., Cross, J.N., Cai, W.J., 2014b. Carbon biogeochemistry of the western Arctic: primary production, carbon export and the controls on ocean acidification. In: Grebeiner, J.M., Maslowski, W. (Eds.), *The Pacific Arctic Region: Ecosystem Status and Trends in a Rapidly Changing Environment*. Springer Science+Business Media, Dordrecht, pp. 223–268.
- Mathis, J.T., Cross, J.N., Evans, W., Doney, S.C., 2015. Ocean acidification in the surface waters of the Pacific-Arctic boundary regions. *Oceanography* 28 (2),

- 122–135. <http://dx.doi.org/10.5670/oceanog.2015.36>.
- Millero, F.J., 1995. Thermodynamics of the carbon-dioxide system in the oceans. *Geochim. Cosmochim. Acta* 59, 661–677.
- Millero, F.J., Zhang, J.Z., Lee, K., Campbell, D.M., 1993. Titration alkalinity of seawater. *Mar. Chem.* 44, 153–165.
- Mucci, A., 1983. The solubility of calcite and aragonite in seawater at various salinities, temperatures, and one atmosphere total pressure. *Am. J. Sci.* 283, 780–799.
- Ono, T., Watanabe, S., Okuda, K., Fukasawa, M., 1998. Distribution of total carbonate and related properties in the North Pacific along 30°N. *J. Geophys. Res. Oceans* 103, 30873–30883.
- Orr, J.C., Fabry, V.J., Aumont, O., Bopp, L., Doney, S.C., Feely, R.A., Gnanadesikan, A., Gruber, N., Ishida, A., Joos, F., Key, R.M., Lindsay, K., Maier-Reimer, E., Matear, R., Monfray, P., Mouchet, A., Najjar, R.G., Plattner, G.K., Rodgers, K.B., Sabine, C.L., Sarmiento, J.L., Schlitzer, R., Slater, R.D., Totterdell, I.J., Weirig, M.F., Yamanaka, Y., Yool, A., 2005. Anthropogenic ocean acidification over the twenty-first century and its impact on calcifying organisms. *Nature* 437, 681–686.
- Rykaczewski, R.R., Dunne, J.P., 2010. Enhanced nutrient supply to the California Current Ecosystem with global warming and increased stratification in an earth system model. *Geophys. Res. Lett.* 37 (21), L21606. <http://dx.doi.org/10.1029/2010GL045019>.
- Siedlecki, S.A., Kaplan, I., Herman, A.J., Nguyen, T.T., Bond, N.A., Newton, J.A., Williams, G.D., Peterson, W.T., Alin, S.R., Feely, R.A., 2016. Experiments with seasonal forecasts of ocean conditions for the northern region of the California Current upwelling system. *Sci. Rep.* 6, 27203. <http://dx.doi.org/10.1038/srep/27203>.
- Somero, G.N., Beers, J., Chan, F., Hill, T., Klinger, T., Litvin, S., 2016. What changes in the carbonate system, oxygen, and temperature portend for the northeastern Pacific Ocean: a physiological perspective. *Bioscience* 66, 14–26. <http://dx.doi.org/10.1093/biosci/biv162>.
- Thomson, R.E., Krassovski, M.V., 2010. Poleward reach of the California undercurrent extension. *J. Geophys. Res.* 115, C09027. <http://dx.doi.org/10.1029/2010JC006280>.
- Thomson, R.E., Hickey, B.M., LeBond, P.H., 1989. In: Beamish, R.J., McFarlane, G. (Eds.), *The Vancouver Island Coastal Current: Fisheries Barrier and Conduit, Effects of Ocean Variability on Recruitment and an Evaluation of Parameters Used in Stock Assessment Models*, vol. 108. Dept. of Fish. and Oceans, Ottawa, Ont., Canada, pp. 265–296.
- Turi, G., Lachkar, Z., Gruber, N., Munnich, M., 2016. Climatic modulation of recent trends in ocean acidification in the California Current System. *Environ. Res. Lett.* 11, 014007. <http://dx.doi.org/10.1088/1748-9326/11/1/014007>.
- UNESCO, 1994. *Protocols for the Joint Global Ocean Flux Study (JGOFS) Core Measurements*. United Nations Educational, Scientific, and Cultural Organization. <http://dx.doi.org/10.1038/NCLIMATE2479>.
- G.G., Hales, B., Langdon, C.J., Haley, B.A., Schrader, P., Brunner, E.L., Gray, M.W., Miller, C.A., Gimenez, I., 2015. Saturation-state sensitivity of marine bivalve larvae to ocean 709 acidification. *Nature Clim. Change* 5, 273–280. [http://ijgofs.who.edu/Publications/Report\\_Series/JGOFS\\_19.pdf](http://ijgofs.who.edu/Publications/Report_Series/JGOFS_19.pdf). Waldbusser.
- Waldbusser, G.G., Hales, B., Langdon, C.J., Haley, B.A., Schrader, P., Brunner, E.L., Gray, M.W., Miller, C.A., Gimenez, I., 2015. Saturation state sensitivity of marine bivalve larvae to ocean acidification. *Nat. Clim. Change* 5, 273–280. <http://dx.doi.org/10.1038/nclimate2479>.
- Weisberg, S.B., Bednaršek, N., Feely, R.A., Chan, F., Boehm, A.B., Sutula, M., Ruesink, J.L., Hales, B., Largier, J.L., Newton, J.A., 2016. Water quality criteria for an acidifying ocean: challenges and opportunities. *Ocean. Coast. Manag.* 126, 31–41. <http://dx.doi.org/10.1016/j.ocecoaman.2016.03.010>.
- Wood, H.L., Spicer, J.L., Widdicombe, S., 2008. Ocean acidification may increase calcification rates, but at a cost. *Proc. R. Soc. B* 275, 1767–1773.
- Wootton, J.T., Pfister, C.A., Forester, J.D., 2008. Dynamic patterns and ecological impacts of declining ocean pH in a high-resolution multi-year dataset. *Proc. Natl. Acad. Sci. U. S. A.* 105, 18848–18853.